

Moisture-induced Anti-plasticization of Polylactic Acid: Experiments and Modeling

Yu Chen, Tian Tang, Cagri Ayranci**

Y. Chen, Dr. T. Tang, Dr. C. Ayranci

Department of Mechanical Engineering, University of Alberta, Edmonton, Alberta, T6G 2R3,
Canada

Emails: tian.tang@ualberta.ca, cayranci@ualberta.ca

Keywords: viscoelasticity, moisture, polylactic acid, plasticization, anti-plasticization

Abstract

Poly(lactic acid) (PLA) is a biodegradable polymer derived from bio-renewable resources. The effect of diffused water molecules on the mechanical properties of PLA, before the onset of hydrolytic degradation, has been rarely studied. In this work, PLA fibers produced by melt-extrusion were conditioned in chambers with different levels of relative humidity (36%, 75%, and 98%), as well as immersed in distilled water. Creep tests were conducted on dry and conditioned samples and creep compliances were extracted. With the increase of moisture content, the decrease in instantaneous elastic compliance, as well as the more flattened curves in the last stage of the creep tests, indicates the existence of water-bridge-anti-plasticization effect. The modified Burgers-Reimschuessel model developed in our previous work is found to be able to predict the effect of absorbed moisture on the viscoelasticity of PLA. The present work highlights the importance of

considering the moisture's anti-plasticization effect. The proposed methodology can be adopted to evaluate the effect of moisture on the viscoelasticity of PLA for different applications.

1 Introduction

Poly(lactic acid) (PLA) is an environmental-friendly polymer derived from bio-renewable resources such as corn starch, potato and sugar cane.^[1] According to a report produced by Grand View Research, the market size of PLA had a value of \$525.47 million USD in 2020 and is expected to have an annual growth rate of 18.1% in the next 8 years.^[2] The reason behind this large demand is the broad range of applications of PLA originating from the various advantages it offers. Firstly, PLA is biocompatible, in that, it is non-toxic, and does not cause immunological rejection when in contact with a living system.^[3] Thus, PLA is a natural choice for biomedical applications such as cardiovascular stents or sutures.^[4] Secondly, PLA has good melt-processability. Traditional melt-based thermoplastic processing technologies, such as extrusion, injection molding and compression molding, can be used for PLA based product manufacturing.^[1] Perhaps, one of the most important advantages of PLA is its biodegradability. PLA can be degraded by first inducing hydrolysis reaction of its ester bonds, followed by exposure to moisture, oxygen and natural microorganisms which decompose it into water, carbon dioxide and a small amount of other non-toxic substances.^[1,4,5] All these advantages make PLA an ideal alternative to petroleum-based polymers that are conventionally used in thermoplastics industry.^[1] PLA has already been commercially utilized in food packaging,^[6] bottles,^[7] biomedical devices^[8] and products in textile, transport and agriculture industries.^[5]

On the other hand, the most important advantage of PLA also leads to a major challenge during its applications. The ester groups in the molecular structure of PLA can be hydrolyzed by water molecules even at room temperature, which eventually leads to the start of biodegradation.^[4] Several studies reported that PLA has a water contact angle of around 75°, suggesting that PLA is hydrophilic in nature.^[9–12] The polar ester groups contribute to the hydrophilicity of PLA, making it susceptible to moisture absorption throughout its service life.^[13] It has been shown that moisture absorption can significantly affect the viscoelastic behavior of PLA,^[8,14] which may result in potential catastrophic failure of PLA products such as biomedical scaffold in biomedical applications, fibers in textile industry and structural components in transportation industry.^[5,8,15] Therefore, the effect of moisture on the viscoelastic properties of PLA should be carefully studied, documented and considered during the product design.^[8,15]

A number of studies have assessed and outlined the mechanism of hydrolytic degradation of PLA.^[4–6,8,16–20] Various parameters that affect hydrolytic degradation, including temperature, humidity, pH, presences of infills, etc. have been reported.^[17,20] Holm et al.^[6] and Niaounakis et al.^[17] studied the effect of hydrolytic degradation on the tensile properties of PLA including Young's modulus, tensile strength and elongation at break. Both works reported that all three properties decreased with hydrolytic degradation. Singh et al.^[8] modeled the viscoelastic constitutive relation of PLA under the influence of hydrolytic degradation. A nonlinear standard solid model proposed by Khan et al.^[21] was used and the change of model parameters during degradation was provided.^[8] The proposed model was validated against tensile test results for PLA degraded for up to 150 days.^[8]

Prior to hydrolytic degradation, significant diffusion of moisture into the PLA has to occur first. Niaounakis et al.^[17] found negligible degradation when PLA was placed under room

temperature (20°C) and 80% relative humidity (RH) for 130 days. Similar conclusion was drawn by Siparsky et al.^[22] from the observation that the time scale for hydrolytic degradation was four to six orders of magnitude larger than that of moisture diffusion. Schmitt et al.^[23] reported that, similar to other hydrophilic polymers, the water molecules that diffused into the PLA also existed in two forms, free water and bound water. Free water means those water molecules that are not attached to the polymer chains and hence are able to move freely within the polymer network.^[24] These molecules tend to form clusters, increasing the inter-chain distance and the free volume within the polymer network.^[25] As a result, the molecular mobility of the polymer chains is enhanced, causing the material to be softened (i.e., plasticized). On the contrary, bound water molecules are attached to the polymer chains through the formation of hydrogen bonds. Additionally, they can establish bridges between polymer chains and therefore restrain their molecular mobility.^[26-28] This so-called water-bridge-anti-plasticization (WBAP) effect has been found in a variety of hydrophilic polymers.^[28-31] The two opposite effects, plasticization caused by free water and anti-plasticization caused by bound water, were discussed and modeled in a recent work.^[29] The model was validated against the experimental results of Onogi et al.^[32] for four different hydrophilic polymers, namely, polyvinyl alcohol (PVA) with degree of polymerization (DP) 600, PVA with DP 2060, Nylon 6 and heat-treated Nylon 6.

Compared to the studies on hydrolytic degradation, the effect of diffused water molecules on the mechanical properties of PLA, before the onset of hydrolytic degradation, has been limited. Zakir et al.^[15] conditioned melt-drawn PLA fibers in four different levels of relative humidity (0%, 35%, 75% and 98%) for four weeks to obtain PLA fibers with different moisture content. They discovered that both Young's modulus and tensile strength of PLA fibers only slightly decreased with increased moisture content.^[15] Algarni et al.^[33] conducted tensile tests on 3D-printed PLA

samples. While the moisture content had little effect on the Young's modulus, the tensile strength slightly increased with moisture content which was in contrast to the results of Zakir et al.^[15] Widiastuti et al.^[34,35] studied the viscoelastic properties of 10 wt% potato starch infilled PLA and proposed an empirical model, using polynomials and fractions, for how the viscoelastic parameters changed with moisture content. The error from the model prediction increased drastically (up to 25% discrepancy) when the moisture content increased from 2 wt% to 6 wt%. Therefore, to the best of our knowledge, the effect of diffused moisture on the viscoelastic behavior of PLA before hydrolytic degradation is poorly studied, and discrepancies remain among the existing literatures.

The objective of the present study is to fill the knowledge gap by proposing a methodology for comprehensive evaluation of the effect of diffused moisture on the viscoelastic constitutive relation of PLA, prior to hydrolytic degradation. We expect that the results can be applied to the design of PLA products for a variety of applications such as food packing, bio-medical devices, and structural components. In addition, the experimental methodology and model developed in this study can be applied to other hydrophilic polymers whose viscoelastic behavior is sensitive to moisture.

2 Methodology

2.1 Preparation of PLA fiber samples

PLA fibers were produced by melt-extrusion. PLA grade 4043D pellets were provided by NatureWorks LLC, USA, which has a number-average molecular weight (M_n) of 106,000 g/mol, polydispersity index of 1.6, and D-lactic acid content from 4.5 wt% to 5 wt%.^[36] According to the manufacturer provided instructions, PLA pellets were firstly dried under vacuum at 80°C for 8 hours (in a Lindberg/Blue MTM vacuum oven - Thermo Fisher Scientific, USA). Then, a

Brabender™ single screw extruder attached to ATR Plasti-Corder drive system (C.W. Brabender Instruments, Inc., Germany), Filabot™ FB00626 air path and Filabot™ FB00073 filament spooler (Triex LLC, USA) were used for fiber production as shown in **Figure 1**. The diameter of the nozzle was 3 mm. Based on manufacturer provided data, the temperature for heating zones 1 and 2 was set to 180°C while the temperature for heating zones 3 and 4 was set to 175°C. The extrusion speed was approximately 1.5 g/min. Fibers with 0.5 ± 0.02 mm diameter were produced. Fiber diameter was chosen based on balancing the considerations of moisture conditioning (thick fibers require longer conditioning time) and creep tests (creep tests are difficult to conduct on thin fibers).

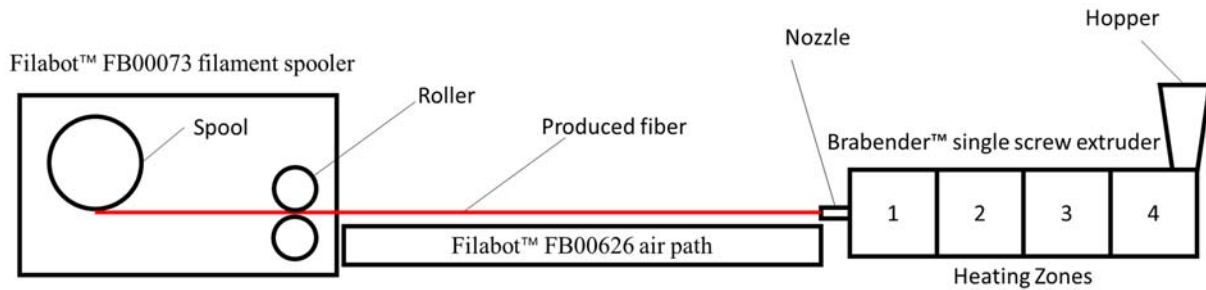


Figure 1. Schematic of the fiber production process

2.2 Sample conditioning and moisture absorption measurement

The produced PLA fibers were firstly placed in Lindberg/Blue M™ vacuum oven at 60°C for 48 hours to release the moisture absorbed during extrusion. They were then cut into approximately 80 mm in lengths for moisture absorption tests under different conditions. The conditioning environments include chambers with different RH levels (36%, 75%, 98%) and immersion in distilled water, all at 20°C. The different RH levels were achieved by placing saturated salt solutions ($\text{MgCl}_2 \cdot 6\text{H}_2\text{O}$ for 36%, NaCl for 75% and K_2SO_4 for 98%) within the conditioning chambers according to ASTM E104-20.^[37] Under each condition, moisture absorption

was measured for seven identical samples using a scale with a precision of 0.1 mg. The samples were periodically removed from the conditioning chamber and weighed.

The moisture content $C(t)$ at each measurement time t was calculated by the following equation^[6,15]

$$C(t) = \frac{m(t) - m(t = 0)}{m(t = 0)} \times 100\% \quad (1)$$

where $m(t)$ is the mass of the sample at time t , $m(t = 0)$ is the weight of the dry sample. For a specific time t , statistics for $C(t)$ were collected from the seven identical samples. The moisture absorption curves were reported as the moisture content C plotted against the square root of time (\sqrt{t}). The conditioning period was 50 days since all the samples reached the saturation level, which is the equilibrium moisture content C_e , within that period. Assuming that the moisture diffusion in the PLA fibers follows Fick's law, the diffusivity D can be estimated by:^[15,38,39]

$$D = \frac{\pi d^2}{16C_e^2} \times k^2 \quad (2)$$

where d is the diameter of the fiber and k the slope of the initial linear portion of the moisture absorption curve.

2.3 Creep tests

After C_e is reached, tensile creep tests were conducted for 15 min to extract the creep compliance. To enhance the grip and minimize the stress concentration, at the two ends of the fiber, paper tabs shown in

Figure 2 were used during the tensile creep tests according to ASTM D3822.^[40] Each fiber sample was glued by poly(ethylene-vinyl acetate) using a glue gun (Topelek, China), onto a paper tab with a gauge length of 40 mm as shown in

Figure 2. All creep tests were conducted immediately after the fibers were taken from the conditioning chamber. During the tests, temperature was approximately 23°C and RH was around 20%. A universal tensile testing system (ElectroForce 3200 Series III, Bose Corporation, USA) equipped with a 10 N load cell was used for all the creep tests.

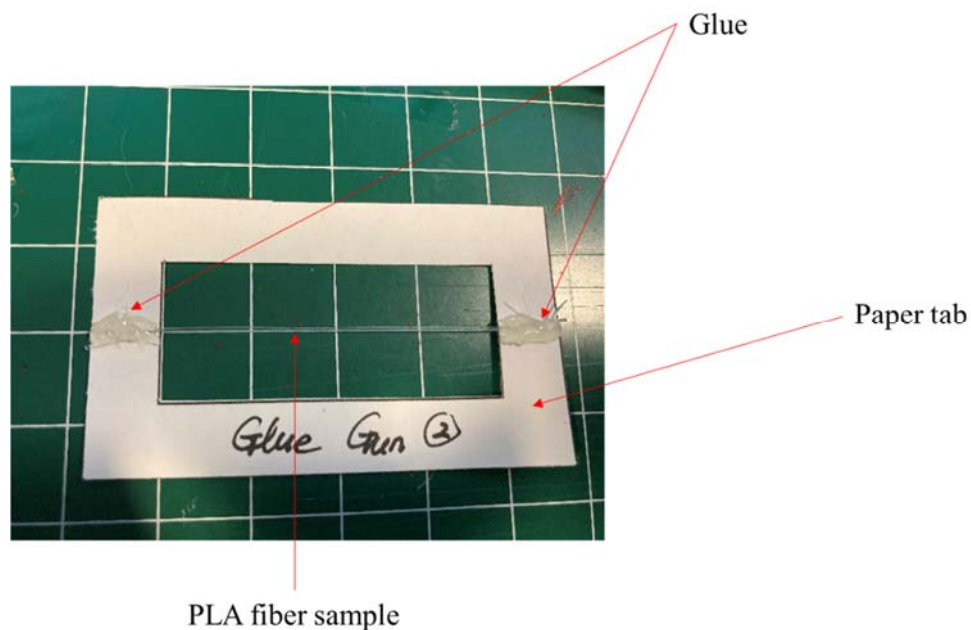


Figure 2. Mounting of the conditioned PLA fiber samples for tensile creep tests

A series of creep tests were first conducted with different applied instantaneous stresses σ_0 in order to obtain the linear viscoelastic limits.^[41] It was discovered that, regardless of C_e , the creep compliance did not change with σ_0 if $\sigma_0 \leq 8$ MPa. 8 MPa was therefore chosen as the applied stress for the remaining tests, so as to limit the material to the linear viscoelastic regime. According to

ASTM D2990,^[42] the stress was programmed to be applied rapidly within 1 s. For each C_e , tests were performed on 5 replicas. The creep compliance was measured every 50 s during the test and the average values over the 5 samples were reported.

2.4 Extracting moisture-dependent viscoelastic parameters

A modified Burgers-Reimschuessel model proposed in our previous work^[29] was used to investigate the effect of diffused moisture on the viscoelastic properties of PLA. This model is briefly introduced here for the ease of access of the readers.

In this model, the constitutive relation of PLA is described by the Burgers model shown in **Figure 3**^[35,43]. E_1 and E_2 are elastic parameters, μ_1 and μ_2 are viscous parameters, and $\varepsilon(t)$ and $\sigma(t)$ are time-dependent strain and stress, respectively. During a creep test, an instantaneous stress σ_0 is applied at time $t = 0$ and the strain response $\varepsilon(t)$ is measured. The creep compliance is the ratio between $\varepsilon(t)$ and σ_0 , which for the Burgers model is given by

$$J(t) = \frac{t}{\mu_2} + \frac{1}{E_2} + \frac{1}{E_1} \left(1 - e^{-\frac{E_1 t}{\mu_1}} \right), \quad t \geq 0 \quad (3)$$

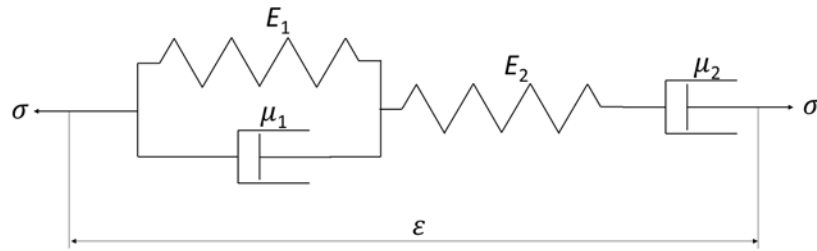


Figure 3. Schematic of Burgers model.

The effect of absorbed moisture is represented by the change of Burgers model parameters P (E_1 , E_2 , μ_1 , or μ_2) with respect to C_e . The modified Burgers-Reimschuessel model^[29] proposed the following dependence of P on C_e

$$P(C_e) = P_f + (P_0 - P_f) \exp(-k_p C_e) + (k_A C_e) \exp(-k_D C_e) \quad (4)$$

where P_0 is value of the parameter for the dry polymer and P_f is the limiting value when C_e is large. k_p is a non-negative constant that describes the exponential decay due to the plasticization by free water; k_A and k_D are non-negative constants introduced to describe the WBAP effect by the last term in **Equation (4)**. This term scales linearly with C_e when it is small, representing stiffening effect from water bridges, while decays at large C_e due to the breaking of water bridges caused by excessive water clusters.

3 Results and Discussion

3.1 Moisture absorption and diffusivity

The moisture absorption curves of the PLA fiber samples under different conditions are presented in **Figure 4**. Under all conditions, rapid moisture uptake is observed within the first two weeks of conditioning, and the increasing trend is almost linear with \sqrt{t} . The rate of increase slows down after these two weeks, and the moisture content reaches the equilibrium values C_e after approximately 35 days. C_e increases with increasing RH level and samples immersed in distilled-water has the maximum. These curves are typical Fickian absorption curves which describe the free diffusion of water molecules without other physical-chemical processes, such as hydrolytic degradation.^[24]

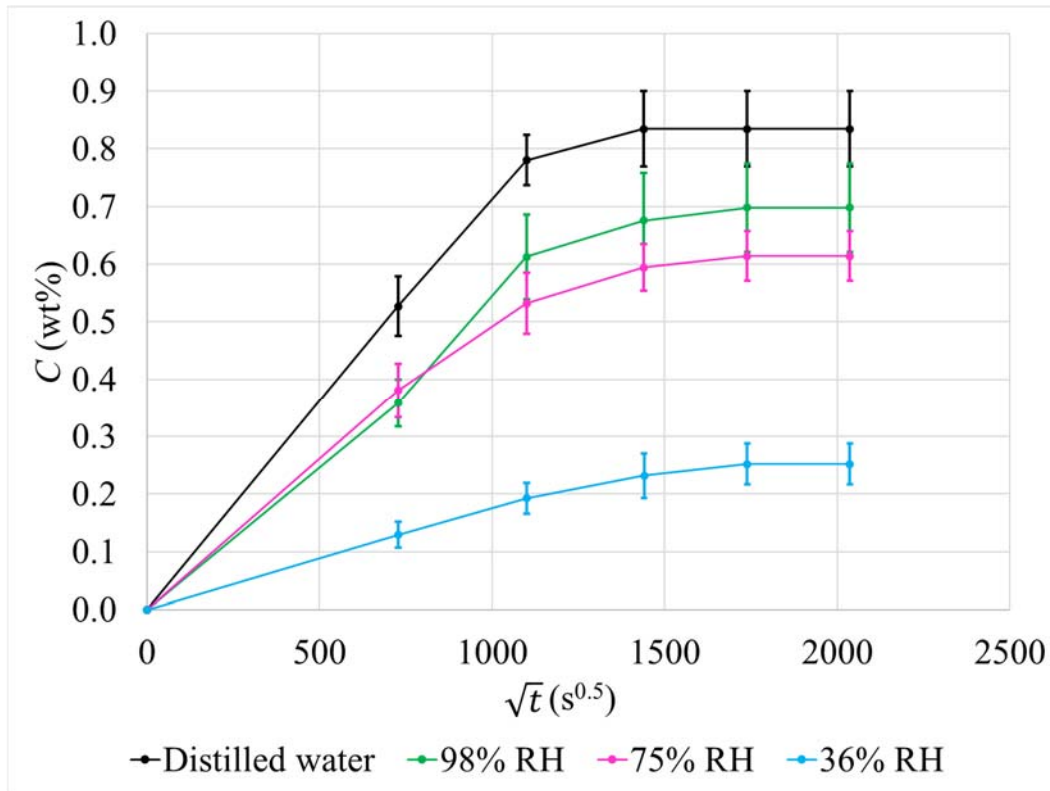


Figure 4. Moisture absorption curves.

Since the characteristics of diffusion follows the Fick's law, **Equation (2)** was used to calculate the diffusivity of water in PLA fibers.^[38] The values of C_e and calculated diffusivity D are listed in **Table 1**. Due to the limited number of data points acquired in the initial linear part of the moisture absorption curves (**Figure 4**), the calculated diffusivity values vary slightly under different conditions. Also, the diffusivity is larger compared to the range reported by Zakir et al.^[15], between 3.1×10^{-17} and 4.6×10^{-15} m²/s. The difference might be attributed to the differences in manufacturing process, crystallinity, and grade of the PLA raw materials.^[44]

Table 1. Equilibrium moisture content and calculated diffusivity

Condition	Equilibrium moisture content C_e (wt%)	Diffusivity D ($\times 10^{-14}$ m ² /s)
Distilled-water	0.835	3.59
98% RH	0.698	2.91
75% RH	0.614	3.20
36% RH	0.252	2.38
Average		3.02

3.2 Creep compliance

The creep compliances under different C_e are plotted in **Figure 5** (a)-(e), which exhibit the typical creep behavior of a semi-crystalline polymer.^[45] **Equation (3)** Error! Reference source not found. was used to fit the data in **Figure 5**, and the extracted Burgers model parameters are plotted against C_e in **Figure 6** (red dots). Then, Equation (4) was used to fit the data in **Figure 6** to capture the moisture dependence of Burgers model parameters. Due to the lack of data in the high C_e regime, the limiting values P_f were all assigned 0. The other parameters in Equation (4) obtained from the fitting and the adjusted R^2 values are shown in

Table 2. P_0 of the four parameters are close to the results obtained by Widiastuti et al.,^[35] indicating that the fitting is physically reasonable. The initial increasing trend of P with respect to C_e confirmed the existence of the anti-plasticization effect. The results from the model fitting are presented by the blue curves in **Figure 6**, and the predictions of the creep compliance using parameters in

Table 2 are shown in **Figure 5** (solid curves). Clearly, the modified Burgers-Reimschuessel model^[29] is able to predict the effect of absorbed moisture on the viscoelasticity of PLA.

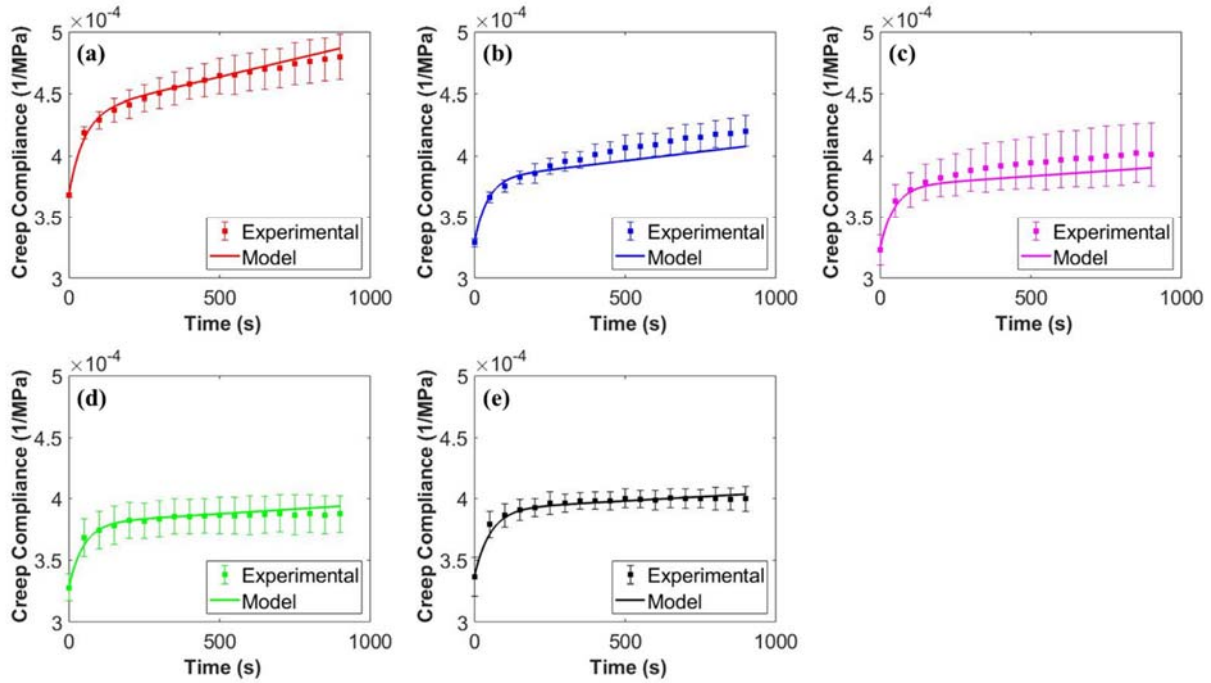


Figure 5. Creep compliance and modeling of PLA with different C_e : (a) dry samples; (b) samples conditioned in 36% RH, $C_e = 0.252$ wt%; (c) samples conditioned in 75% RH, $C_e = 0.614$ wt%; (d) samples conditioned in 98% RH, $C_e = 0.698$ wt%; (e) samples immersed in distilled water, $C_e = 0.835$ wt%.

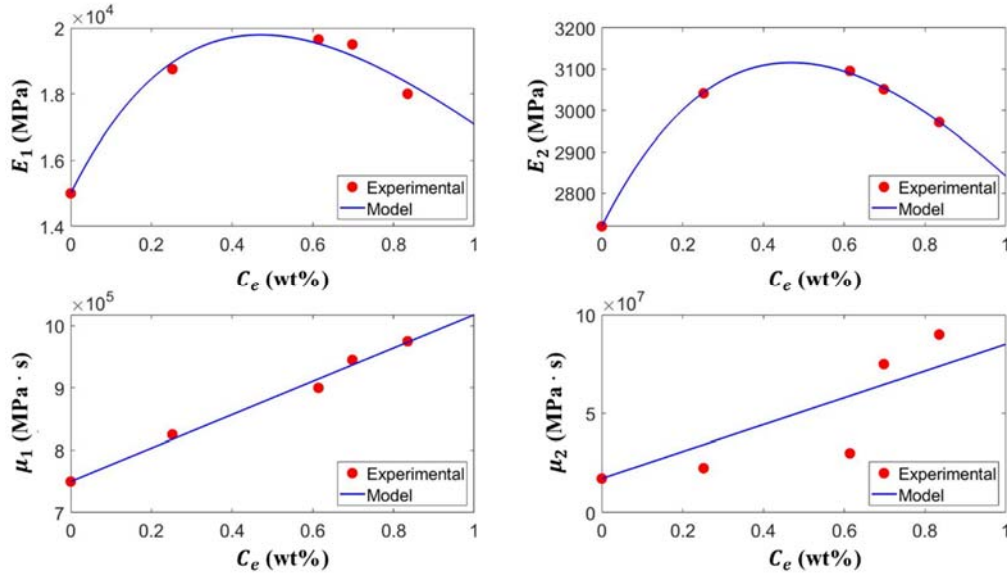


Figure 6. Change of Burgers model parameters with respect to C_e (red dots) as well as the fitting using the modified Burgers-Reimschuessel model (blue curves)

Table 2. Fitted model parameters and quality of fitting

Parameter	P_0 (Unit)	P_f (Unit)	k_p (1/%)	k_A (Unit/%)	k_D (1/%)	Adjusted R^2
E_1 (MPa)	15000	0	1.214	42640	1.217	0.96014
E_2 (MPa)	2719.5	0	0.921	4449	0.928	0.99889
μ_1 (MPa · s)	7.5×10^5	0	0	2.677×10^5	0	0.99012
μ_2 (MPa · s)	1.725×10^7	0	0	6.782×10^7	0	0.69524

3.3 Discussion

As shown in Figure 5, the instantaneous elastic compliance (at $t = 0$) decreases from $3.7 \times 10^{-4} \text{ MPa}^{-1}$ to $3.3 \times 10^{-4} \text{ MPa}^{-1}$ when C_e increases from 0 to 0.252 wt%. In addition, with the increase of C_e , the creep compliance curves are more flattened in the last stage of the creep test.

Both phenomena indicate that with more absorbed moisture the material is more resistive to external load, which can be explained by the WBAP effect.^[29] Using Equation (4) and the parameters in

Table 2, it can be calculated that for $C_e < 1$ wt%, the term that corresponds to plasticization $[P_f + (P_0 - P_f) \exp(-k_p C_e)]$ is significantly smaller than the anti-plasticization term $[(k_A C_e) \exp(-k_D C_e)]$. This further confirms that a significant portion of water molecules were forming water bridges which stiffened the material. The viscoelasticity of hydrophilic polymers with moisture content less than 1 wt% was never characterized in the literature. Onogi et al.^[32] and Widiastuti et al.^[35] only characterized viscoelasticity of PVA, Nylon 6 and 10 wt% potato starch reinforced PLA with moisture content more than 1.4 wt%. Thus, to the best of our knowledge, the anti-plasticization effect of water molecules on PLA was firstly characterized and modeled in this work.

Comparing Figure 5 (d) and (e), the creep compliance of the samples immersed in distilled water is slightly higher than those conditioned under 98% RH, although C_e is higher for samples immersed in distilled water. The additional moisture in the samples immersed in distilled water did not stiffen the material, instead, it slightly plasticized the material. The reason is believed to be the different forms of water molecules on the boundary of the polymers during conditioning. According to Fan^[24], the difference between water immersion and conditioning in a high RH

environment is the state of water on the boundary between hydrophilic polymers and the environment. For polymers immersed in water, the water molecules enter as clusters while for polymers conditioned in a high RH environment, water molecules enter as individual molecules. Therefore, it is easier for water-bridges to be formed in the samples conditioned under high humidity, whereas water clusters tend to cause plasticization and soften the material.

Tsuji and Muramatsu^[46] also characterized the tensile properties of pure PLA films before and after water immersion. In their work, the tensile strength and Young's modulus both decreased slightly after water immersion while the elongation at break slightly increased. In other words, the PLA films were slightly plasticized by water absorption, and no anti-plasticization was observed. The difference from the present study is likely caused by the larger amount of water absorbed by PLA in Tsuji and Muramatsu (around 4 wt%), as compared to 0.835 wt% in this work after immersing PLA in distilled water. The different C_e achieved by water immersion might be caused by the different PLA raw materials (LACTY[®]5000 in Tsuji and Muramatsu vs. NatureWorks 4043D in this work), as well as the different sample preparation techniques (solution casting and melt-quenching in Tsuji and Muramatsu vs. melt-extrusion in this work).

In **Figure 6**, within the range of C_e obtained in this work, the elastic parameters (E_1 and E_2) firstly increase and then slightly decrease as C_e is increasing. The transition between the increasing and decreasing trends occurs at approximately 0.4 wt% of moisture content. However, the viscous parameters (μ_1 and μ_2) increase monotonically with C_e . One possible explanation is that when $C_e \geq 0.4$ wt%, small free water clusters might have already formed, which could break the existing water bridges and weaken the WBAP effect. The weakening appears to be more strongly reflected in the elastic parameters. These parameters represent the recoverability of the polymer chains from a deformed state and are affected by the interactions between polymer chain

coils, including those arising from the water bridges.^[29,47-49] Breaking of the water bridges by the small water clusters could weaken the recoverability, thus causing a decrease in the elastic parameters. The viscous parameters capture the resistance when polymer chains slide past one another.^[48,50] They tend to increase with the amount of inter-chain non-covalent bonds, including water bridges while decrease with the free volume within the material.^[29,47,50] While the small water clusters could reduce the interaction established by water bridges, they might also fill the existing free volumes and provide extra barriers for molecular chains to slide under external load.^[31] These two competing factors could then reduce the impact of small water clusters on the viscous parameters.

The results presented in this paper provide strong evidence of water's anti-plasticization effect and the model is a useful tool for the prediction of change in the PLA's mechanical behaviors due to this effect. PLA has been used as micro-actuators^[51] and substrates for sensors^[52] in micro-electromechanical systems (MEMS). In these applications, a minor change in the mechanical behavior of the materials can significantly change the deformation of the components, which in turn changes the performances of these MEMs products.^[31,53-55] Therefore, during the design of these products, it is essential to evaluate and predict the mechanical behavior of the PLA components. The experimental methodology and model presented in this paper provide a useful tool for this purpose.

4 Conclusion

In this work, the effect of diffused moisture on the viscoelastic behavior of PLA was evaluated. Different equilibrium moisture content C_e was achieved by conditioning PLA samples

under different RH or immersing them in distilled water. The modified Burgers-Reimschuessel model proposed by our group^[29] was shown to be able to predict the creep compliance of the conditioned PLA samples with good accuracy. The experimental results here provided evidence on the stiffening effect of water molecules where they form bridges between the molecular chains. The present work highlights the importance of considering the water's anti-plasticization effect when evaluating the effect of moisture on the mechanical properties of hydrophilic polymers. The methodology used in this paper can also be adopted to evaluate the effect of moisture on the viscoelasticity of other hydrophilic polymers in different applications.

Acknowledgements

This work was supported by Alberta Innovates (AB Innovat BFM-18-002 Ayranci), and Discovery Grants (NSERC RGPIN-2018-06309 (Ayranci), NSERC RGPIN-2018-04281 (Tang)) from the Natural Sciences and Engineering Research Council of Canada.

Received: ((will be filled in by the editorial staff))

Revised: ((will be filled in by the editorial staff))

Published online: ((will be filled in by the editorial staff))

5 References

- [1] E. Castro-aguirre, F. Iñiguez-franco, H. Samsudin, X. Fang, R. Auras, *Adv. Drug Delivery Rev.* **2016**, *107*, 333.
- [2] *Polylactic Acid Market Size, Share & Trends Analysis Report By End-Use (Packaging, Textile, Agriculture, Automotive & Transport, Electronics), By Region (North America, APAC, Europe), And Segment Forecasts, 2021 - 2028*, **2021**.
- [3] Y. Ramot, M. Haim-Zada, A. J. Domb, A. Nyska, *Adv. Drug Delivery Rev.* **2016**, *107*, 153.
- [4] R. Auras, L. Lim, Susan E. M. Selke, H. Tsuji, *Polylactic Acid, Synthesis, Structures, Properties, Processing, and Applications*, John Wiley And Sons, Hoboken, **2010**.
- [5] N. F. Zaaba, M. Jaafar, *Polym. Eng. Sci.* **2020**, *60*, 2061.
- [6] V. K. Holm, S. Ndoni, J. Risbo, *J. Food Sci.* **2006**, *71*, 40.
- [7] R. A. Cairncross, J. G. Becker, S. Ramaswamy, R. O'Connor, *Appl. Biochem. Biotechnol.* **2006**, *131*, 774.
- [8] A. Singh, R. M. Guedes, D. Paiva, F. D. Magalhães, *SN Appl. Sci.* **2020**, *2*, 1.
- [9] S. M. Bhasney, R. Patwa, A. Kumar, V. Katiyar, *J. Appl. Polym. Sci.* **2017**, *134*, 45390.
- [10] V. Marturano, V. Bizzarro, V. Ambrogi, A. Cutignano, G. Tommonaro, G. R. Abbamondi, M. Giamberini, B. Tylkowski, C. Carfagna, P. Cerruti, *Polymers* **2019**, *11*, 68.
- [11] A. Orue, A. Eceiza, C. Peña-Rodríguez, A. Arbelaiz, *Materials* **2016**, *9*, 400.

- [12] M. Esmacili, G. Pircheraghi, R. Bagheri, V. Altstädt, *Polym. Adv. Technol.* **2019**, *30*, 839.
- [13] M. Pannico, P. la Manna, *Front. Chem.* **2019**, *7*, 1.
- [14] I. Widiastuti, I. Sbarski, S. H. Masood, *J. Appl. Polym. Sci.* **2013**, *127*, 2654.
- [15] K. M. Zakir, A. J. Parsons, C. D. Rudd, I. Ahmed, W. Thielemans, *Eur. Polym. J.* **2014**, *53*, 270.
- [16] E. C. L. Angela M. Harris, *J. Appl. Polym. Sci.* **2008**, *107*, 2246.
- [17] M. Niaounakis, E. Kontou, M. Xanthis, *J. Appl. Polym. Sci.* **2011**, *119*, 472.
- [18] D. Moreno Nieto, M. Alonso-García, M.-A. Pardo-Vicente, L. Rodríguez-Parada, *Polymers* **2021**, *13*, 1036.
- [19] P. Kakanuru, K. Pochiraju, *Addit. Manuf.* **2020**, *36*, 101529.
- [20] S. Farah, D. G. Anderson, R. Langer, *Adv. Drug Delivery Rev.* **2016**, *107*, 367.
- [21] A. S. Khan, O. Lopez-Pamies, R. Kazmi, *Int. J. Plast.* **2006**, *22*, 581.
- [22] G. L. Siparsky, K. J. Voorhees, J. R. Dorgan, K. Schilling, *J. Environ. Polym. Degrad.* **1997**, *5*, 125.
- [23] E. A. Schmitt, D. R. Flanagan, R. J. Linhardt, *Macromolecules* **1994**, *27*, 743.
- [24] X. Fan, in *Int. Conf. Therm. Mech. Multi-Phys. Simul. Exp. Microelectron. Microsyst. EuroSimE 2018*, Freiburg, **2008**.
- [25] H. Fujita, A. Kishimoto, *J. Polym Sci.* **1958**, *28*, 569.
- [26] B. Yang, W. M. Huang, C. Li, L. Li, *Polymer* **2006**, *47*, 1348.

- [27] R. M. Hodge, G. H. Edward, G. P. Simon, *Polymer* **1996**, 37, 1371.
- [28] H. K. Reimschuessel, *J. Polym. Sci., Part A: Polym. Chem.* **1978**, 16, 1229.
- [29] Y. Chen, C. Ayranci, T. Tang, *Modified Burgers-Reimschuessel Model for Moisture-Sensitive Polymers*, Accepted by Journal of Polymer Science, **2021**.
- [30] A. Ishisaka, M. Kawagoe, *J. Appl. Polym. Sci.* **2004**, 93, 560.
- [31] S. Schmid, S. Kühne, C. Hierold, *J. Micromech. Microeng.* **2009**, 19.
- [32] S. Onogi, K. Sasaguri, T. Adachi, S. Ogihara, *J. Polym. Sci.* **1962**, 58, 1.
- [33] M. Algarni, *Polymers* **2021**, 13, 1.
- [34] I. Widiastuti, I. Sbarski, S. H. Masood, *J. Appl. Polym. Sci.* **2014**, 131, 1.
- [35] I. Widiastuti, I. Sbarski, S. H. Masood, *Mech. Time Depend. Mater.* **2014**, 18, 387.
- [36] E. H. Backes, L. de N. Pires, L. C. Costa, F. R. Passador, L. A. Pessan, *J. Compos. Sci.* **2019**, 3, 52.
- [37] *ASTM E104-20 Standard Practice for Maintaining Constant Relative Humidity by Means of Aqueous Solutions*, **2020**.
- [38] J. Crank, *The Mathematics of Diffusion*, Oxford University Press, London, **1975**.
- [39] Y. Y. Leu, W. S. Chow, *J. Vinyl Addit. Technol.* **2011**, 17, 40.
- [40] *ASTM D3822-14 (2020) Standard Test Method for Tensile Properties of Single Textile Fibers*, **2020**.
- [41] O. Starkova, A. Aniskevich, *Mech. Time Depend. Mater.* **2007**, 11, 111.

- [42] *ASTM D2990-17 Standard Test Methods for Tensile, Compressive, and Flexure Creep and Creep-Rupture of Plastics*, **2017**.
- [43] J. Dong, C. Mei, J. Han, S. Lee, Q. Wu, *Addit. Manuf.* **2019**, 28, 621.
- [44] M. Drieskens, R. Peeters, J. Mullens, D. Franco, P. J. Lemstra, D. G. Hristova-Bogaerds, *J. Polym. Sci., Part B: Polym. Phys.* **2009**, 47, 2247.
- [45] W. N. Findley, *Creep and Relaxation of Nonlinear Viscoelastic Materials: With an Introduction to Linear Viscoelasticity*, Dover Publications Inc., New York, **1989**.
- [46] H. Tsuji, H. Muramatsu, *J. Appl. Polym. Sci.* **2001**, 81, 2151.
- [47] U. W. Gedde, *Polymer Physics*, Springer, Dordrecht, **1999**.
- [48] W. D. Callister, D. G. Rethwisch, *Material Science and Engineering, An Introduction*, John Wiley & Sons, Inc., Hoboken, USA, **2010**.
- [49] L.H. Sperling, *Introduction to Physical Polymer Science*, John Wiley & Sons, Inc, **2006**.
- [50] M. T. Shaw, W. J. MacKnight, *Introduction to Polymer Viscoelasticity*, John Wiley & Sons, Inc., Hoboken, **2005**.
- [51] S. Amaya, S. Sugiyama, in *Transducers & Eurosensors XXVII: The 17th International Conference on Solid-State Sensors, Actuators and Microsystems* , **2013**.
- [52] A. V. Quintero, N. Frolet, D. Marki, A. Murette, G. Mattana, D. Briand, N. F. de Rooij, in *Proceedings of the IEEE International Conference on Micro Electro Mechanical Systems (MEMS)*, Institute Of Electrical And Electronics Engineers Inc., **2014**, pp. 532–535.

- [53] C. J. Robin, K. N. Jonnalagadda, *J. Micromech. Microeng.* **2016**, 26, DOI 10.1088/0960-1317/26/2/025020.
- [54] K. B. Lee, *Principles of Microelectromechanical Systems*, WILEY, **2010**.
- [55] C. C. Nguyen, V. K. T. Ngo, H. Q. Le, W. L. Li, *Microsyst. Technol.* **2019**, 25, 2767.